2017

Effects of Crab Cavity Multipoles on JLEIC Ion Ring Dynamic Aperature

S. I. Sosa
Old Dominion University

V. S. Morozov
Thomas Jefferson National Accelerator Facility

S. U. DeSilva
Old Dominion University

J. R. Delayen
Old Dominion University

Repository Citation

Sosa, S. I.; Morozov, V. S.; DeSilva, S. U.; and Delayen, J. R., "Effects of Crab Cavity Multipoles on JLEIC Ion Ring Dynamic Aperature" (2017). *Physics Faculty Publications*. 328.
https://digitalcommons.odu.edu/physics_fac_pubs/328

Original Publication Citation

Sosa Guitron, S., De Silva, S., Delayen, J., & Morozov, V. (2017). *Effects of crab cavitiy multipoles on JLEIC ion ring dynamic aperture.* Paper presented at the 8th International Particle Accelerator Conference, Copenhagen, Denmark. https://doi.org/10.18429/JACoW-IPAC2017-WEPIK044

EFFECTS OF CRAB CAVITIY MULTIPOLES ON JLEIC ION RING DYNAMIC APERTURE *

S. I. Sosa†[1,2], V. S. Morozov[2], S. U. De Silva[1,2], J. R. Delayen[1,2]
[1]Center for Accelerator Science, Old Dominion University, Norfolk, VA 23529, USA
[2]Thomas Jefferson National Accelerator Facility, Newport News, VA 23606, USA

Abstract

We study the effects of crab cavity multipole fields on the beam dynamic aperture of the Jefferson Lab Electron-Ion Collider (JLEIC) ion ring. Crab cavities are needed to compensate for luminosity loss due to a 50 mrad crossing angle at the interaction point. New compact crab cavity designs are interesting as they do not require considerable space in the ring but their non-linear field needs to be well understood. In this contribution, we study the impact of field multipoles on the beam dynamic aperture and report tolerance values for crab cavity multipoles.

INTRODUCTION

In order to achieve the high luminosity requirement at JLEIC, the current ion ring design implements a crabbing scheme to compensate for geometric luminosity loss due to a 50 mrad crossing angle at the interaction point (IP) [1]. In a local crabbing scheme, rf deflecting crab cavities are placed at both sides of the IP, excluding potential crab-induced effects from the rest of the ring. With the appropriate voltage and phase advance, the upstream crab cavity imparts a longitudinally dependent transverse kick, of opposite signs on the head and tail of a bunch, so as to recover a frontal collision at IP. The downstream cavity gives a kick at an opposite sign to compensate the initial kick. The fields produced by the crab cavity depend on its particular geometry and are non-linear in nature. A multipole treatment of the fields is used to describe non-linearities. Detailed analytical treatment of the crab cavity multipole fields can be found in [2] and [3]. Particularly, the n-th order multipole will produce a horizontal momentum change

$$\Delta p_x^{(n)} = q x^{n-1} b_n, \tag{1}$$

with q the particle charge, x the horizontal position of a particle with respect to the bunch center, and b_n are the multipole field strengths. Using a standard definition for magnets, b_n are calculated as

$$b_n = \int_{-\infty}^{\infty} B^{(n)}(z)dz, \quad [T/m^{n-2}], \tag{2}$$

With

$$B^{(n)}(z) = \frac{1}{(n-1)!}\frac{\partial^{n-1}By}{\partial x^{n-1}}, \tag{3}$$

the n-th term in the field multipole expansion. A change in momentum $\Delta p_x^{(n)}$ will get particles deflected by

$$\Delta x'_{(n)} = \frac{\Delta p_x^{(n)}}{p_z} = \frac{q}{\gamma m \beta c} x^{n-1} b_n. \tag{4}$$

Cavity Model in Elegant

Crab cavities with multipole components up to $n = 5$ are implemented in *elegant* [4] using Multipole RF DeFlector (MRFDF) elements. This element changes the momentum of a particle by

$$\Delta p_x = \frac{e}{\omega}\sum_{n=1}^{5} n b_n x^{n-1}\cos\phi_n \tag{5}$$

with a deflection $\Delta x' = \Delta p_x/p_z$. In this expression, $b_n = b_n[V/m^n]$. From Eqs. (1) and (5), a relation

$$b_n\left[\frac{V}{m^n}\right] = b_n\left[\frac{T}{m^{n-2}}\right]\cdot\frac{\omega}{n} \tag{6}$$

is determined. Different multipoles can be assigned independent amplitude and phase values.

Ion Ring Model

The ion ring collision optics is shown in Fig. 1. Its design includes chromaticity compensation blocks (CCB) at each side of the IP. The CCB locations are ideal for crab cavities to be placed, as the phase advance is right and β_x values are high, thus requiring a lower crabbing voltage. This lattice is described in [5]. The crabbing parameters are shown in Table 1.

Table 1: Crabbing Parameters of JLEIC Ion Ring Model

Parameter	Proton	Units
Energy	100	GeV
Frequency	952.6	MHz
Crossing Angle	50	mrad
β_x^*	0.1	m
β_x^{crab}	363.44	m
Deflecting Voltage	20.82	MV

DYNAMIC APERTURE ANALYSIS OF CRAB CAVITIES

The dynamic aperture (DA) of 100 GeV proton beam is investigated when crab cavities with multipole field content

---

* Supported in part by the U.S. Department of Energy, Office of Science, Office of Nuclear Physics under contract DE-AC05-06OR23177. The U.S. Government retains a non-exclusive, paid-up, irrevocable, world-wide license to publish or reproduce this manuscript for U.S. Government purposes.

† ssosa006@odu.edu

ISBN 978-3-95450-182-3

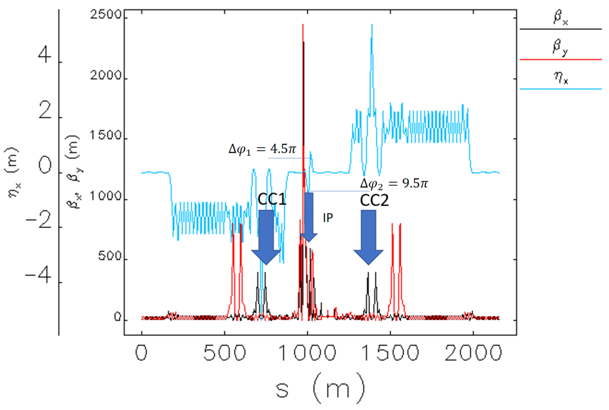

Figure 1: Collision optics of the JLEIC ion ring used in this study. Crab cavities are placed in the inner horizontal CCB locations at each side of the IP, where β_x is high, as indicated by the blue arrows.

are placed at CCB locations in the ion ring. The DA is determined over 2000 turns and scanned in the x-y plane along 55 rays. Strong beam cooling emittance values are assumed, where $\gamma\epsilon_{x/y} = 0.35/0.07$ μm· rad. These values correspond to transverse bunch sizes $\sigma_{x/y} = 0.121/0.154$ mm at the start of the lattice where the DA is determined. The start point is chosen outside the crab region, in a dispersion-free location with $\alpha_{x/y} = 0$ and $\beta_{x/y} = 4.885/32.681$ m.

Pure Dipole Kick

We first study the effect of a crab cavity linear dipole kick, with the phase set to the crab phase, ie, maximum and opposite at the head an tail of the bunch, and zero at the bunch center. Figure 2 shows the beam DA of the ion ring when the crabbing voltage is turned off and on. When the cavity voltage is set to zero, the horizontal aperture is ±90.7 σ_x, but once the cavity is turned to the crabbing voltage, it gets reduced to ±68 σ_x. No considerable effect on the vertical DA is seen.

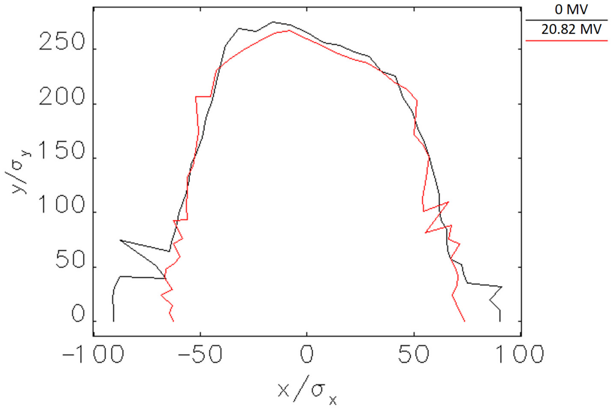

Figure 2: Beam DA of the ion ring with the crab cavity voltage set to 0 and 20.82 MV for comparison. Only a linear kick is considered in this case.

Multipole Field Specifications

Multipole terms with the same phase as the dipole kick are added to the linear kick and varied independently. Table 2 presents values of b_n that when added to the linear kick, reduce the horizontal DA to about ±50 σ_x. This multipole values are combined into a reference cavity, which reduces the ring DA to ±46.2 σ_x, and is used for comparison with crab cavity designs. The signs on the multipole components are chosen to match the signs on the cavity designs shown in Table 3.

Table 2: Normalized Multipole Components that reduce DA to ±50 σ_x.

b_n $\left[\frac{mT/m^{n-2}}{1MV}\right]$	**DA to** $\pm 50\sigma$
b_2	-16.08
b_3	217.12
b_4	321.67
b_5	-0.8×10^5

CRAB CAVITY FOR JLEIC ION RING

Crab cavity design concepts for JLEIC have been reported previously [6,7]. In this contribution, multipoles corresponding to different crab cavity designs, shown in Fig. 3, are used to estimate the impact on the ring DA. These multipole components are determined using *CST Microwave Studio*, and are presented in Tables 3 and 4, together with its corresponding reduced horizontal DA value. Figure 4 shows the DA for all the geometries studied. These results show that both 1-cell and 3-cell cavity designs lie within tolerance. The resulting DA obtained with the 60 and 70 mm aperture cavities appear to be consistent. Multi-cell cavities are particularly attractive as a lower number of cavities are required, for example, for the 3-cell cavity design, only 5 are required per each side of the IP, whereas single-cell designs requires 15 cavities to reach the voltage requirement of 20.82 MV. We also studied two different pole geometries, as shown in Fig. 3. In this case, curved-pole cavities produce a significantly reduced DA, about half of the size produced by flat-pole cavities. Curved-pole cavities reduce the b_3 component at the expense of a small increase in b_5. The observed significant reduction of the DA needs further study.

Table 3: Multipole Components and DA of Crab Cavity Designs

b_n $\left[\frac{mT/m^{n-2}}{1MV}\right]$	**3-cell**		**1-cell**	
	60 mm	70 mm	60 mm	70 mm
b_2 $[\times10^{-4}]$	-3	-3	-5	-5
b_3	697.1	610	853.2	797.5
b_4	0.92	0.63	1.55	1.2
b_5 $[\times10^5]$	-1.1	-5.4	-1.2	-0.44
DA $[\sigma_x]$	±44.1	±47	±45.9	±46.6

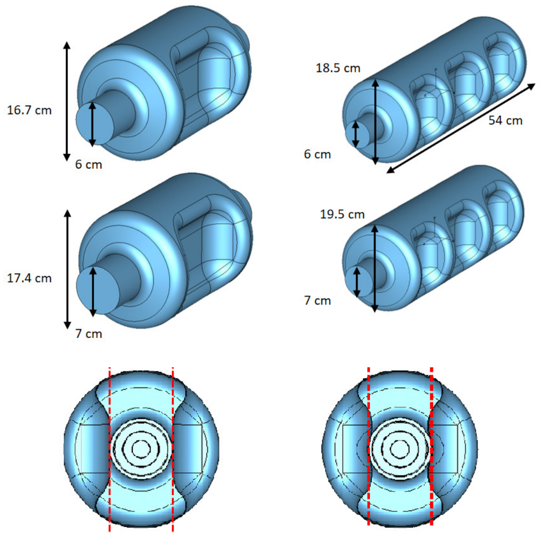

Figure 3: Single-cell and 3-cell crab cavity designs with 60 and 70 mm apertures. The bottom two figures are the cross section of a 3-cell 70 mm cavity with flat (left) and curved (right) poles.

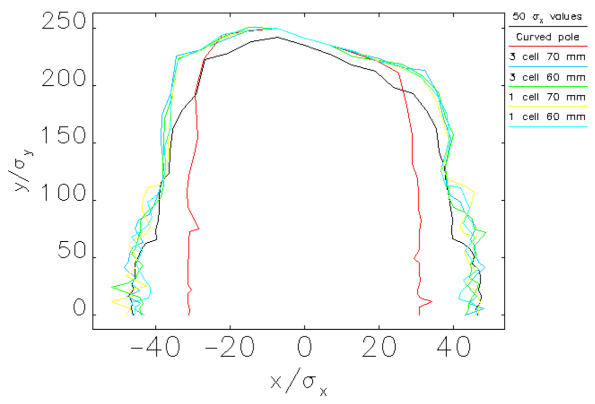

Figure 4: Dynamic aperture comparison between an element with the highest multipole field strengths shown in Table 2 and the cavity designs shown in Fig. 3.

It is important to mention that currently the JLEIC ion ring DA is limited to $\pm 10\sigma$ by the multipole fields of the final focusing quadrupoles (FFQ) [8]. Therefore, the results presented in this contribution suggest that the multipoles from crab cavities are not a limiting DA factor. A complete JLEIC collider DA simulation should include effects from both FFQ multipoles and crab cavity multipoles.

Table 4: Multipole Components of a 3-cell 70 mm Aperture Crab Cavity with Flat and Curved Pole Geometries

$b_n \left[\frac{mT/m^{n-2}}{1MV}\right]$	**3-cell 70mm** Flat	**3-cell 70mm** Curved
$b2$	-3×10^{-4}	-8×10^{-9}
$b3$	610	35.1
$b4$	0.63	-2×10^{-5}
$b5$ [$\times10^5$]	-5.4	-5.7
DA [σ_x]	±47	±30.9

CONCLUSION

Crab cavities with multipole components are used in a working model of the JLEIC ion ring model to study their effects on the ring DA. Multi-cell cavity geometry seems to have a smaller effect on the DA. The largest effect on DA comes from b_5, although higher multipole terms need to be included for a more detailed analysis. The impact on DA from crab cavity multipoles is less than the current limiting effect from final focusing quadrupole multipoles.

REFERENCES

[1] S.Abeyratne *et. al.*, “MEIC Design Summary", January 2015

[2] J. Barranco, et. al, TUPPR027, IPAC2012, New Orleans, LA, USA (2012).

[3] S. U. De Silva and J. R. Delayen, SUPB038, LINAC2012, Tel Aviv, Israel (2012).

[4] M. Borland, “elegant: A Flexible SDDS-Compliant Code for Accelerator Simulation," Advanced Photon Source LS-287, September 2000.

[5] S. Sosa, V. Morozov and J. R. Delayen, WEPIK043, these proceedings.

[6] H. Park, A. Castilla, J. R. Delayen, S. U. De Silva and V. Morozov, WEPMR034, IPAC2016, Busan, Korea (2016).

[7] S. U. De Silva, H. Park, and J. R. Delayen, WEPMW022, IPAC2016, Busan, Korea (2016).

[8] G.H. Wei, V.S. Morozov, F. Lin, Y. Zhang, F. Pilat, THPMR053, IPAC2016, Busan, Korea (2016).

ISBN 978-3-95450-182-3